Parasitol Res (2016) 115:587–595
DOI 10.1007/s00436-015-4775-6

ORIGINAL PAPER

# Upregulated Tim-3/galectin-9 expressions in acute lung injury in a murine malarial model

**Jinfeng Liu**[1,2] · **Siyu Xiao**[1,2] · **Shiguang Huang**[3] · **Fuquan Pei**[4] · **Fangli Lu**[1,2]

Received: 3 August 2015 / Accepted: 1 October 2015 / Published online: 23 October 2015


**Abstract** Malaria is the most relevant parasitic disease worldwide, and severe malaria is characterized by cerebral edema, acute lung injury (ALI), and multiple organ dysfunctions; however, the mechanisms of lung damage need to be better clarified. In this study, we used Kunming outbred mice infected with *Plasmodium berghei* ANKA (*Pb*ANKA) to elucidate the profiles of T cell immunoglobulin and mucin domain-3 (Tim-3) and its ligand galecin-9 (Gal-9) in the development of ALI. Mice were injected intraperitoneally with $10^6$ *Pb*ANKA-infected red blood cells. The lungs and mediastinal lymph nodes (MLNs) were harvested at days 5, 10, 15, and 20 post infections (p.i.). The grade of lung injury was histopathologically evaluated. Tim-3- and Gal-9-positive cells in the lungs and MLNs were stained by immunohistochemistry, and the messenger RNA (mRNA) expressions of Tim-3, Gal-9, and related cytokines were assessed using quantitative real-time polymerase chain reaction (qRT-PCR). Bronchoalveolar lavage fluid (BALF) analyses were performed from days 18 to 20 p.i. The results showed that the pathological severities in the lungs were increased with times and the total protein level in the BALFs was significantly elevated in *Pb*ANKA-infected mice. The numbers of Gal-9$^+$ and Tim-3$^+$ cells in the lungs were significantly increased, and the mRNA levels of both Gal-9 and Tim-3 in the lungs and MLNs were over-expressed in *Pb*ANKA-infected mice. In conclusion, our data suggested that Tim-3/Gal-9 may play a role in *Pb*ANKA-induced ALI.

**Keywords** *Plasmodium berghei* · Mice · Acute lung injury · Tim-3 · Galecin-9

✉ Shiguang Huang
thshg@126.com

✉ Fangli Lu
fanglilu@yahoo.com

[1] Department of Parasitology, Zhongshan School of Medicine, Sun Yat-sen University, Guangzhou 510080, China

[2] Key Laboratory of Tropical Disease Control (Sun Yat-sen University), Ministry of Education, Guangzhou 510080, China

[3] School of Medicine, Jinan University, Guangzhou 510632, China

[4] Guangdong Provincial Center for Disease Control and Prevention, Guangzhou 511430, China

## Introduction

Malaria is a common infection in the world. *Plasmodium* infection may result in severe malaria in patients infected with *Plasmodium falciparum*, *Plasmodium vivax*, and *Plasmodium knowlesi*, which can develop malaria-associated acute lung injury/acute respiratory distress syndrome (ALI/ARDS) and often results in morbidity and mortality. ALI or ARDS is with mortality rates of approximately 80 % (Taylor et al. 2012; White et al. 2013), accompanied by pulmonary edema (Taylor et al. 2006). Malaria-associated ALI/ARDS is thought to be due, in part, to increased alveolar permeability, parasite sequestration, and host immune response; however, the mechanisms behind it are largely unknown (Mohan et al. 2008).

T cell Ig and mucin domain-containing molecules (TIMs) are key regulators of immune responses (Rodriguez-Manzanet et al. 2009). Galectins are a family of highly conserved glycan-binding proteins that play an important role in the innate and adaptive immune responses (Rabinovich and Toscano 2009). Galectin-9 (Gal-9) down-regulates T helper (Th)1 and Th17 responses and is involved in the suppression mediated by CD4$^+$ CD25$^+$ T regulatory (Treg) cells, mainly through interaction with the Th1-specific cell surface molecule TIM-3 (Seki et al. 2008; Chou et al. 2009). The Gal-9/

Tim-3 interaction acts as a specific inhibitor of Th1 and Th17 immune responses (Lu et al. 2015). Although the participation of lungs involved in the severity of malaria has been well documented (Boulos et al. 1993; Taylor et al. 2006; Rojo-Marcos et al. 2008), knowledge about this pathogenesis is still limited. The mechanisms through which infection with *Plasmodium* spp. result in lung disease are largely unknown.

This study sought to explore the expressions of Tim-3/Gal-9 in the development of ALI induced by *Plasmodium berghei* infection in a mouse model; we suppose that their interaction may play an important role in the pathogenesis of ALI in the experimental malarial mice.

## Materials and methods

### Mice and experimental infections

Kunming (KM, outbred) mice were obtained from the Animal Center of Sun Yat-sen University. Female KM mice (6–8 weeks old) and *P. berghei* ANKA (*Pb*ANKA) were used throughout the study, maintained in specific-pathogen-free environment, and had free access to a commercial basal diet and tap water ad libitum. Animals were provided with humane care and healthful conditions during their stay in the facility. A total of 42 mice were included, in which 38 mice were injected intraperitoneally (i.p.) with $10^6$ *Pb*ANKA-infected red blood cells (iRBCs) and 4 mice were injected with equal volume of phosphate-buffered saline (PBS) as negative controls. Mortality was monitored daily. Four *Pb*ANKA-infected mice were sacrificed by $CO_2$ asphyxiation for examination at days 5, 10, 15, and 20 post infections (p.i.), respectively, and the remained 22 *Pb*ANKA-infected mice were used for survival observation. The protocol in this study was approved by the Committee on the Ethics of Animal Experiments of the Sun Yat-sen University.

### BALF analysis

Bronchoalveolar lavage fluids (BALFs) were obtained by instillation and aspiration of 0.6 ml aliquots of PBS from *Pb*ANKA-infected mice between days 18 to 22 p.i. prior to death after infection, and uninfected controls were sacrificed at the same time. The BALFs were spun at 800*g* at 4 °C for 5 min, and the supernatants were stored at −80 °C for further analysis. Total protein concentrations of the BALFs were measured using a BCA protein assay (Sigma-Aldrich).

### Parasitemia

Parasitemia developments in *Pb*ANKA-infected mice were monitored daily by microscopic examination of Giemsa-stained thin blood smears of tail blood. Parasitemia was determined by counting the Giemsa-positive cells with the aid of a hand counter, and more than 1000 RBCs were counted by microscopy (×100) to determine the percentage of parasitized RBCs.

### Histopathology

For histopathological analysis, the lungs and mediastinal lymph nodes (MLNs) from *Pb*ANKA-infected mice were harvested and immediately fixed in 10 % buffered natural formaldehyde (Guangzhou Chemical Reagent Factory, China) for 48 h. Four-micrometer-thick sections (50- or 100-μm distance between sections) of the organs from each mouse, stained with hematoxylin and eosin (H&E) (Sigma-Aldrich), were evaluated for histological changes. Sections were analyzed by a pathologist who was blinded for groups. To score lung inflammation and damage, the lung pathology was semiquantitatively scored as described previously (Knapp et al. 2004) with minor modification. In brief, the following parameters were analyzed: interstitial inflammation, intra-alveolar inflammation, bronchitis, alveolar edema, endothelialitis, and thrombi formation. Each parameter was graded on a scale from 0 to 3 as follows: 0, absent; 1, mild; 2, moderate; and 3, severe. The total lung inflammation score was expressed as the sum of the scores for each parameter and the maximum being 18.

### Immunohistochemical staining for Tim-3 and Gal-9 in the lungs and MLNs

Immunohistochemistry was carried out using the streptavidin–biotin–peroxidase complex (SABC) method. Tissue sections (5-μm) were deparaffinized and rehydrated in distilled water. Heat-induced antigen retrieval was carried out in an 800-W microwave oven for 30 min. Endogenous peroxidase activity was blocked by incubation with 3 % hydrogen peroxide in methanol for 10 min at 37 °C. Nonspecific binding was blocked by incubation in 10 % normal goat serum in 1 % bovine serum albumin (Sigma-Aldrich)–PBS (pH 7.4) for 10 min at room temperature. Sections were incubated with rabbit anti-Tim-3 (Wuhan Boster Biological Engineering Co., Ltd., China) (1:200 dilutions) and anti-Gal-9 (Beijing Bioss Biological Co., Ltd, China) (1:400 dilutions) overnight at 4 °C, and sections incubated with secondary antibodies only were used as isotype controls. Immunohistochemical staining was then detected with a SABC kit and developed with diaminobenzidine tetrahydrochloride (Zhongshan Golden Bridge Technology, Beijing, China). The sections were counterstained with hematoxylin followed by light microscopy. Tim-3- and Gal-9-positive cells were identified by dark-brown staining.

### Morphometric analysis

Immunopositive cells in the lungs and MLNs of *Pb*ANKA-infected mice were quantified by using images of the histologic sections captured with a digital system and analyzed by using Image-Pro Plus (Image Z1 software, Media Cybernetics, MD, US). The number of cells in each field was determined under high-power field as well as the area of each field (0.015066 $mm^2$). The density of positive cells was expressed as the number of cells per square millimeter.

### Measurement of mRNA expression using qRT-PCR

Total RNA was extracted from about 100 mg of the lung and MLN tissues using a RNA Extraction Kit (TaKaRa) according to the manufacturer's protocol. The quality of total RNA was analyzed by running 5 μl of each RNA sample on a 1.0 % agarose gel stained with ethidium bromide. The quantity of total RNA was estimated by measuring the ratio of absorbance at 260 and 280 nm using a NanoDrop ND-1000 spectrophotometer (NanoDrop Technologies). First-strand complementary DNA (cDNA) was constructed from 1.0 μg of total RNA with oligo (dT) as primers using a PrimeScript 1st Strand cDNA Synthesis Kit (TaKaRa) following the manufacturer's protocol. cDNA was stored at −80 °C until use. To determine tissue messenger RNA (mRNA) levels of Tim-3, Gal-9, IL-6, IL-10, and tumor necrosis factor (TNF)-α, quantitative real-time polymerase chain reaction (qRT-PCR) was performed using SYBR Green qPCR Master Mix (TaKaRa) according to the manufacturer's instructions. Primers are listed in Table 1. Briefly, a total of 10 μl reaction mixture contained 5.0 μl of SYBR® Premix Ex Taq™ (2×), 0.5 μl of each primer (10 pM), 3.0 μl of $dH_2O$, and 1.0 μl of cDNA (0.2 μg/μl). Amplification was pre-denaturized for 30 s at 95 °C followed by 43 cycles of 5 s at 95 °C and 20 s at 60 °C with a LightCycler® 480 instrument (Roche Diagnostics). Specific mRNA expressions were normalized to that of the housekeeping gene, β-actin, and the results are expressed as fold change compared to uninfected controls.

### Statistical analysis

Results of experimental studies were reported as mean± SD. Statistical analysis of the data was performed by Wilcoxon rank sum test, Student's *t* test, and one-way ANOVA followed by Bonferroni's multiple comparison tests using SPSS software for Windows (version 19.0; SPSS, Inc., IL). All graphs were performed using GraphPad Prism software, and a value of $P<0.05$ was considered statistically significant.

**Table 1** Primer sequences of mouse target cytokines and housekeeping genes used for quantitative real-time polymerase chain reaction (qRT-PCR) assays

| Genes | Primer sequence (5′ → 3′) | References |
|---|---|---|
| TNF-α | Forward primer CCCTCACACTCAGATCATCTTCT | Zhao et al. (2011) |
| | Reverse primer GCTACGACGTGGGCTACAG | |
| IL-6 | Forward primer CTGATGCTGGTGACAACCAC | Wei et al. (2013) |
| | Reverse primer CAGAATTGCCATTGCACAAC | |
| IL-10 | Forward primer AGCCGGGAAGACAATAACTG | Jones et al. (2010) |
| | Reverse primer CATTTCCGATAAGGCTTGG | |
| Galectin-9 | Forward primer GTTGTCCGAAACACTCAGAT | Reddy et al. (2011) |
| | Reverse primer ATATGATCCACACCGAGAAG | |
| Tim-3 | Forward primer CCACGGAGAGAAATGGTTC | Geng et al. (2006) |
| | Reverse primer CATCAGCCCATGTGGAAAT | |
| β-Actin | Forward primer TGGAATCCTGTGGCATCCATGAAAC | Jones et al. (2010) |
| | Reverse primer TAAAACGCAGCTCAGTAACAGTCCG | |

## Results

### Malaria-associated ALI

The symptoms and parasitemia of mice were monitored daily after *Pb*ANKA injection, and the mice died between 8 and 22 days p.i. As shown in Fig. 1a, approximately 32 % (7/22) of *Pb*ANKA-infected mice succumbed between 8 and 10 days p.i.; the remaining mice died between 15 and 22 days p.i., which mainly due to malaria-related pathologies such as hyperparasitemia, severe anemia, and ALI/ARDS, etc., and the parasitemia reached higher levels (59.4 to 70.2 %) when deaths occurred between 18 and 22 days p.i. (Fig. 1b). Dyspnea or respiratory insufficiency was observed in almost 90 % of the infected mice prior to death between 18 and 22 days p.i. To confirm the model of *Pb*ANKA-induced ALI, bronchoalveolar lavage (BAL) was performed in mice between 18 and 22 days p.i., and the BALFs were examined for protein content. Compared with uninfected controls, the total protein levels in the BALFs were significantly increased at 18−22 days p.i. ($P<0.01$) (Fig. 1c), indicating that a disruption of the alveolar-capillary membrane barrier and ALI occurred as a result of *Pb*ANKA infection.

### Lung and MLN histopathology

The lung tissues of mice were examined histologically. As shown in Fig. 2a, the control sections of lungs from uninfected mice treated with PBS had no obvious morphological or structural abnormalities. However, lung tissue architecture was massively distorted and moderate to severe inflammatory cellular infiltrations (polymorphonuclear cells, lymphocytes, and mononuclear cells) were dispersed in the lung interstitial and alveolar spaces, and alveolar edema, hemorrhage, thickening of the alveolar septum, and highly parasitized RBCs were noted in the lungs of *Pb*ANKA-infected mice at days 5, 10, 15, and 20 p.i. Semiquantitative score standard for severity was made based on pathological changes of the lung tissues in the different times. As shown in Fig. 2b, the pathological severity scores in the lungs of *Pb*ANKA-infected mice at all the times p.i. were significantly higher ($P<0.001$) than those measured in the control mice, and the pathological severity increased as time progressed. Compared with day 5 p.i., there were significantly increased pathological scores in the lungs of *Pb*ANKA-infected mice at days 10 ($P<0.01$), 15 ($P<0.001$), and 20 ($P<0.001$) p.i.; compared with day 10 p.i., there were significantly increased pathological scores in the lungs at days 15 and 20 p.i. ($P<0.001$). Compared with uninfected controls, parasitized RBCs and the loss of normal architecture (cortical and medullary regions) were noted in the MLN sections of *Pb*ANKA-infected mice at days 5, 10, 15, and 20 p.i. (Fig. 2c).

### Immunohistochemical staining for Gal-9- and Tim-3-positive cells in the lungs and MLNs

As shown in Fig. 3a, by immunohistochemistry staining, no Gal-$9^+$ and Tim-$3^+$ cells were observed in the lung tissues of uninfected controls (Fig. 3a (a, b)); however, there were marked increased Gal-$9^+$ and Tim-$3^+$ cells in the lungs of *Pb*ANKA-infected mice at days 5 (Fig. 3a (c, d)), 10 (Fig. 3a (e, f)), 15 (Fig. 3a (g, h)), and 20 (Fig. 3a (i, j)) p.i. Cell counts were performed for the numbers of Gal-9- and Tim-3-positive cells in the lung tissues. As shown in Fig. 3b, compared with uninfected controls, there were significant higher numbers of Gal-$9^+$ cells in the lungs of *Pb*ANKA-infected mice at all the times including days 5 ($P<0.05$), 10 ($P<0.05$), 15 ($P<0.001$), and 20 ($P<0.001$) p.i., and there were significant higher numbers of Tim-$3^+$ cells in the lungs at days 10 ($P<0.001$), 15 ($P<0.001$), and 20 ($P<0.001$) p.i. Compared with day 5 p.i., there was significant higher number of Tim-$3^+$ cells in the lungs at day 10 p.i. ($P<0.01$); compared with day 10 p.i., there were significant higher numbers of both Gal-$9^+$ and Tim-$3^+$ cells in the lungs at days 15 ($P<0.001$ and $P<0.05$, respectively) and 20 ($P<0.001$ and $P<0.05$, respectively) p.i.; the numbers of Tim-$3^+$ cells had no significant differences between days 15 and 20 p.i. ($P>0.05$), but there was significant higher number of Gal-$9^+$ cells in the lungs at day 20 p.i. than that at day 15 p.i. ($P<0.01$).

As shown in Fig. 4a, there were a few Gal-$9^+$ and Tim-$3^+$ cells in the MLN sections of uninfected controls (Fig. 4a (a, b)). However, there were obvious increased Gal-$9^+$ and Tim-$3^+$cells in the MLNs of *Pb*ANKA-infected mice at day 5 p.i. (Fig. 4a (c, d)) and markedly increased Gal-$9^+$ and Tim-$3^+$

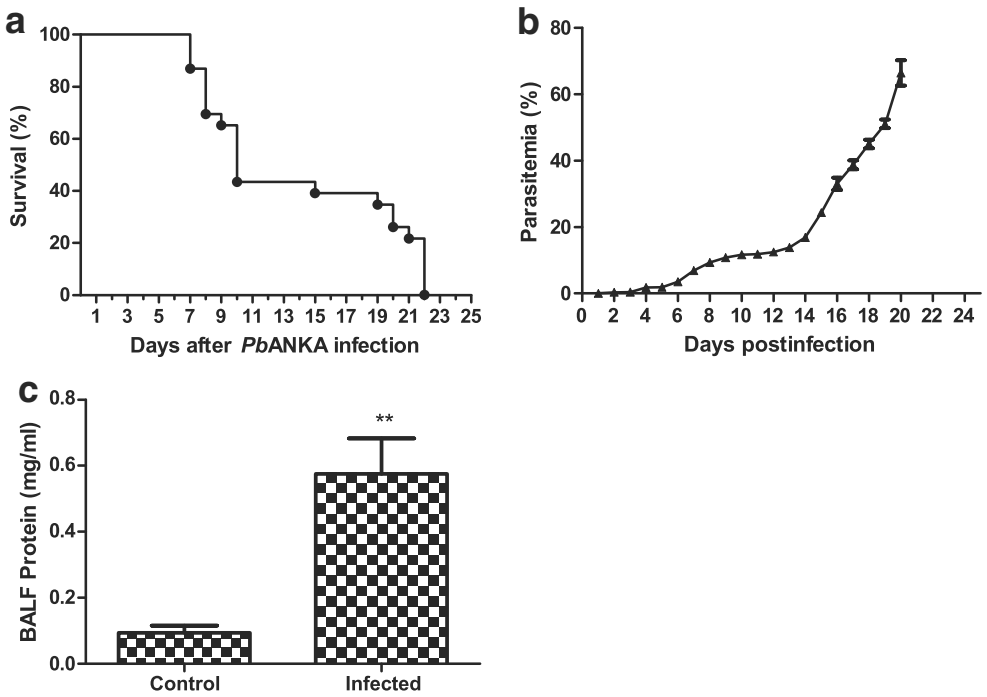


**Fig. 1** Survival rate, parasitemia, and BALF total protein level of *Pb*ANKA-infected mice. **a** Survival curves of mice infected with *Pb*ANKA ($n=22$). The mice died between days 8 and 20 p.i., in which 7 succumbed between days 8 and 10, and 15 died between days 15 and 22. **b** Time course of parasitemia in *Pb*ANKA-infected mice ($n=3$ for each time point). Parasitemias are shown as mean±SD. **c** Measurement of total protein levels in the BALFs from mice infected with *Pb*ANKA. Compared with uninfected controls ($n=4$), the total protein level was significantly increased in the BALF of *Pb*ANKA-infected mice ($n=6$) at 18 - 22 days p.i. (**$P<0.01$)

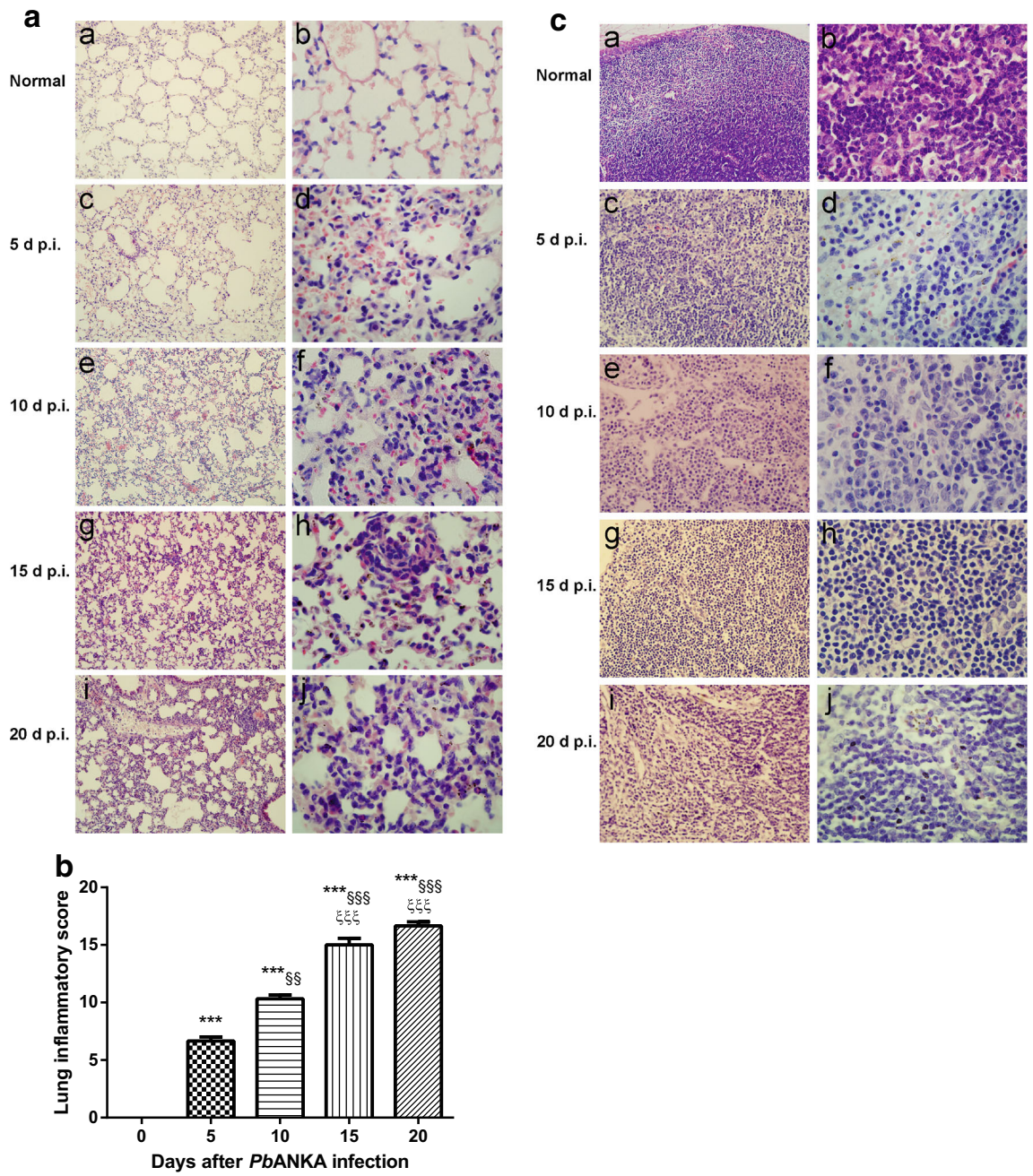


**Fig. 2** Histopathological changes in the lungs and MLNs of *Pb*ANKA-infected mice. **a** Histopathological changes in the lungs. No histological alterations were observed in the lungs of uninfected mice (*a*, *b*); moderate to severe alveolar septum thickening, inflammatory cells penetrating into the lung interstitial and alveolar spaces, edema, and hemorrhage were noted in *Pb*ANKA-infected mice at days 5 (*c*, *d*), 10 (*e*, *f*), 15 (*g*, *h*), and 20 (*i*, *j*) p.i. Original magnification×400 (*a*, *c*, *e*, *g*, *i*); ×1000 (*b*, *d*, *f*, *h*, *j*); H&E stain. **b** Histopathological score analysis of the lungs. Data are represented as mean±SD. Significant differences between groups are analyzed by Wilcoxon rank sum test. $^{**}P<0.01$ and $^{***}P<0.001$ vs control group; §§$P<0.01$ and §§§$P<0.001$ vs 5 days p.i.; ξξ$P<0.01$ and ξξξ$P<0.001$ vs10 days p.i. **c** Histopathological changes in the MLNs. No histological alterations were observed in the MLN of uninfected mice (*a*, *b*); moderate to severe proliferation and activation of inflammatory cells were observed in the MLNs of *Pb*ANKA-infected mice at days 5 (*c*, *d*), 10 (*e*, *f*), 15 (*g*, *h*), and 20 (*i*, *j*) p.i. Original magnification ×400 (*a*, *c*, *e*, *g*, *i*) and ×1000 (*b*, *d*, *f*, *h*, *j*), H&E stain

cells at days 10 (Fig. 4a (e, f)), 15 (Fig. 4a (g, h)), and 20 (Fig. 4a (i, j)) p.i. As shown in Fig. 4b, compared with uninfected controls, the numbers of Gal-9$^+$ and Tim-3$^+$ cells in the MLNs were significant higher at days 10 ($P<0.001$ and $P<0.05$, respectively), 15 ($P<0.001$ and $P<0.01$, respectively), and 20 ($P<0.001$ and $P<0.01$, respectively) p.i. The number of Gal-9$^+$ cells in the MLNs was significantly increased at day 5 p.i. ($P<0.001$) but not that of Tim-3$^+$ cells ($P>0.05$).

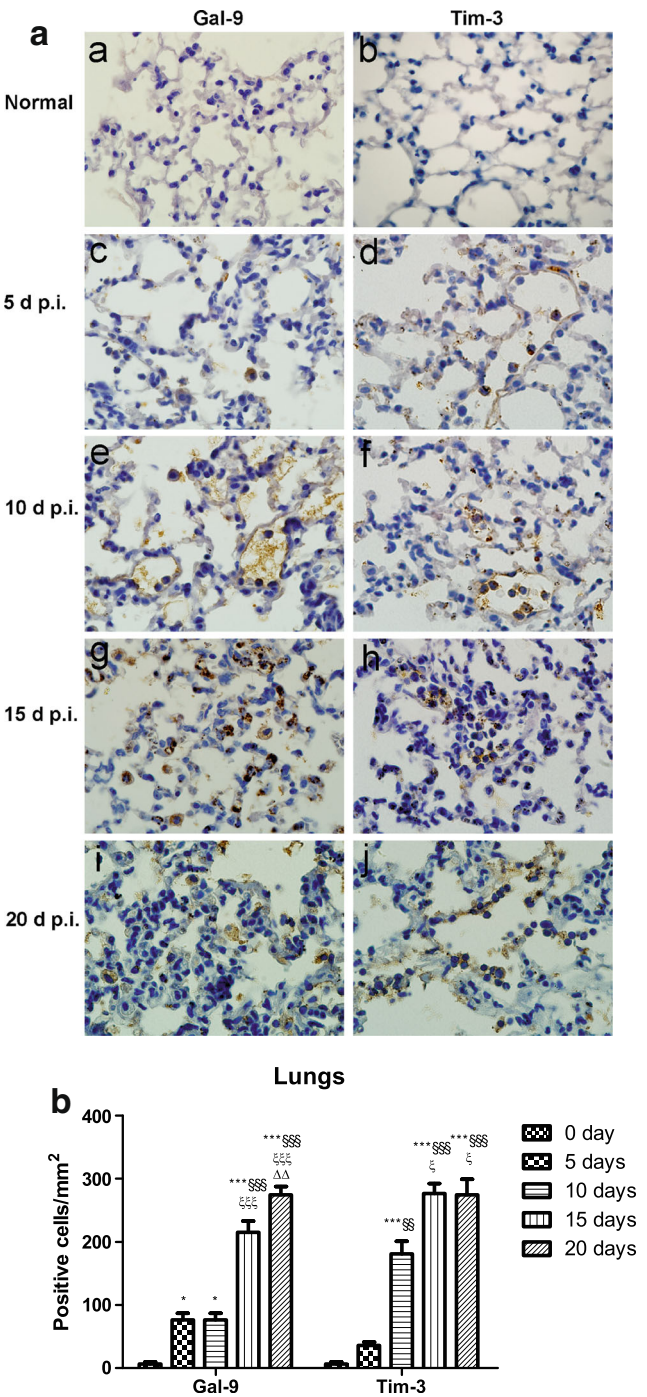


**Fig. 3** Immunohistochemical staining for Gal-9- and Tim-3-positive cells in the lungs of *Pb*ANKA-infected mice. **a** Immunohistochemical staining for Gal-9 and Tim-3 in the lung tissues of uninfected mice (*a*, *b*) and of *Pb*ANKA-infected mice at days 5 (*c*, *d*), 10 (*e*, *f*), 15 (*g*, *h*), and 20 (*i*, *j*) p.i. Original magnification ×1000. **b** Morphometric analysis of Gal-9- and Tim-3-positive cells in the lung tissues. The density of positive cells was expressed as the number of cells per square millimeter. Data are presented as means±SD; experiments were performed with three mice per group. **P*<0.05 and ****P*<0.001 vs control group; §§*P*<0.01 and §§§*P*<0.001 vs 5 days p.i.; ξ*P*<0.05 and ξξξ*P*<0.001 vs 10 days p.i.; ΔΔ*P*<0.01 vs 20 days p.i.

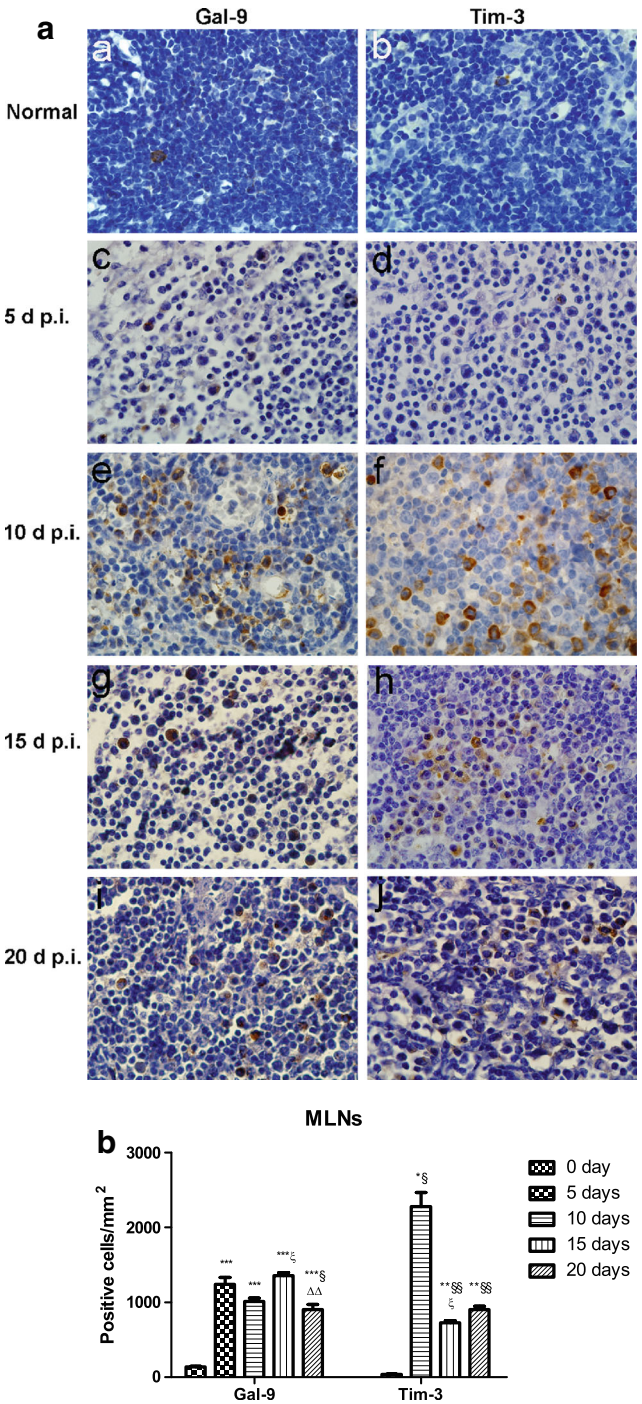


**Fig. 4** Immunohistochemical staining for Tim-3- and Gal-9-positive cells in the MLNs of *Pb*ANKA-infected mice. **a** Immunohistochemical staining for Gal-9 and Tim-3 in the MLN tissues of uninfected mice (*a*, *b*) and of *Pb*ANKA-infected mice at days 5 (*c*, *d*), 10 (*e*, *f*), 15 (*g*, *h*), and 20 (*i*, *j*) p.i. Original magnification ×1000. **b** Morphometric analysis of Gal-9- and Tim-3-positive cells in the MLN tissues. The density of positive cells was expressed as the number of cells per square millimeter. Data are presented as means±SD; experiments were performed with three mice per group. **P*<0.05, ***P*<0.01 and ****P*<0.001 vs control group; §*P*<0.05 and §§*P*<0.01 vs 5 days p.i.; ξ*P*<0.05 vs 10 days p.i.; ΔΔ*P*<0.01 vs 20 days p.i.

Compared with day 10 p.i., there were significantly increased number of Gal-9$^+$ cells ($P<0.05$) and significantly decreased number of Tim-3$^+$ cells ($P<0.05$) in the MLNs at day 15 p.i.; compared with day 15 p.i., the number of Gal-9$^+$ cells was significantly decreased at day 20 p.i. ($P<0.01$); however, the numbers of Tim-3$^+$ cells had no significant difference between days 15 and 20 p.i. ($P>0.05$).

### Gal-9 and Tim-3 mRNA expressions in the lungs and MLNs

To further confirm the expressions of Gal-9 and Tim-3 in immune cells, the mRNA expressions of Gal-9 and Tim-3 in the lungs and MLNs were detected by using qRT-PCR. As shown in Fig. 5a, b, compared with uninfected controls, Gal-9 mRNA expressions were significantly increased in the lungs of *Pb*ANKA-infected mice at days 5 ($P<0.001$), 10 ($P<0.01$), 15 ($P<0.05$), and 20 ($P<0.001$) p.i. and were significantly increased in the MLNs at days 15 ($P<0.05$) and 20 ($P<0.001$) p.i. Compared with day 5 p.i., Gal-9 levels in the lungs were significantly decreased at days 10 ($P<0.05$) and 15 ($P<0.01$) p.i.; compared with day 15 p.i., Gal-9 levels in the lungs and MLNs were significantly increased at day 20 p.i. ($P<0.001$ and $P<0.05$, respectively). Compared with uninfected controls, Tim-3 mRNA expressions in the lungs and MLNs of *Pb*ANKA-infected mice were significantly increased at days 10 ($P<0.05$), 15 ($P<0.01$), and 20 ($P<0.001$ and $P<0.01$, respectively) p.i.; compared with day 5 p.i., Tim-3 levels in the lungs and MLNs were significantly increased at days 10 ($P<0.01$ and $P<0.05$, respectively), 15 ($P<0.001$ and $P<0.01$, respectively), and 20 ($P<0.001$ and $P<0.01$, respectively) p.i.; Tim-3 levels in both the lungs and MLNs had no significant differences between days 10 and 15 p.i. ($P>0.05$); however, compared with day 15 p.i., Tim-3 level in the lungs was significantly increased at day 20 p.i. ($P<0.05$).

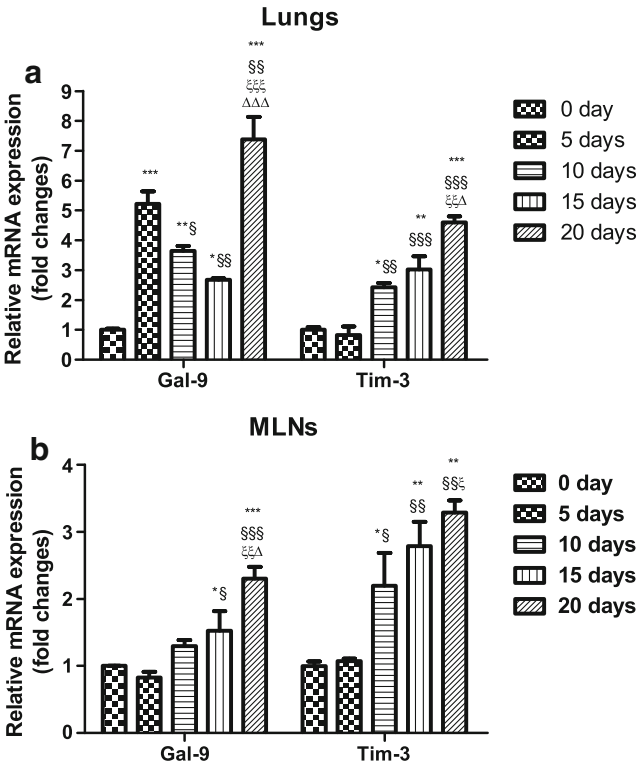


**Fig. 5** mRNA expressions of Tim-3 and Gal-9 in the lung (**a**) and MLN (**b**) tissues of *Pb*ANKA-infected mice by qRT-PCR. Values are means from triplicate measurements, and data are presented as means ±SD; two independent experiments were performed with four mice per group. *$P<0.05$; **$P<0.01$ and ***$P<0.001$ vs control group; §$P<0.05$; §§$P<0.01$, and §§§$P<0.001$ vs 5 days p.i.; ξ$P<0.05$; ξξ$P<0.01$; and ξξξ$P<0.001$ vs 10 days p.i.; Δ$P<0.05$ and ΔΔΔ$P<0.001$ vs 15 days p.i.

### Determination of pro- and anti-inflammatory cytokine responses in the lungs and MLNs

To fully understand the immunologic mechanisms in the development of ALI in *Pb*ANKA-infected mice, the cytokine responses were evaluated by measuring pro-inflammatory (TNF-α and IL-6) and anti-inflammatory cytokine (IL-10) mRNA expressions in the lungs and MLNs by using qRT-PCR. As shown in Fig. 6a, b, compared with uninfected

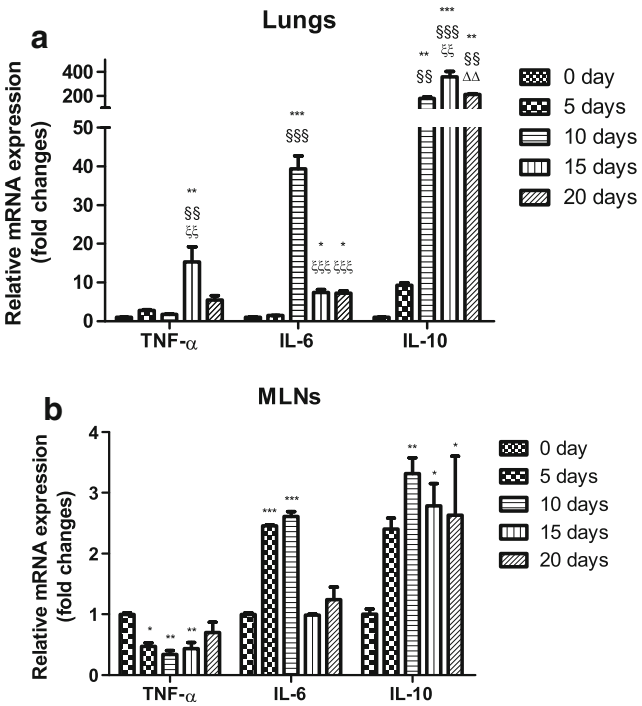


**Fig. 6** Cytokine (TNF-α, IL-6, and IL-10) mRNA expressions in the lung (**a**) and MLN (**b**) tissues of *Pb*ANKA-infected mice by qRT-PCR. Values are means from triplicate measurements, and data are presented as means±SD; two independent experiments were performed with four mice per group. *$P<0.05$; **$P<0.01$, and ***$P<0.001$ vs control group; §§$P<0.01$, and §§§$P<0.001$ vs 5 days p.i; ξξ$P<0.01$, and ξξξ$P<0.001$ vs 10 days p.i; ΔΔ$P<0.01$ vs 15 days p.i.

controls, TNF-α expressions in the lungs of *Pb*ANKA-infected mice were significantly increased at day 15 ($P<0.01$) but significantly decreased in the MLNs at days 5 ($P<0.05$), 10 ($P<0.01$), and 20 ($P<0.01$) p.i. Compared with uninfected controls, IL-6 expressions were significantly increased in the lungs at days 10 ($P<0.001$), 15 ($P<0.05$), and 20 ($P<0.05$) p.i. but significantly decreased at days 15 ($P<0.001$) and 20 ($P<0.001$) p.i. in comparison of day 10 p.i.; IL-6 expressions were significantly increased in the MLNs at days 5 and 10 p.i. ($P<0.001$); IL-10 expressions were significantly increased in the lungs and MLNs at days 10 ($P<0.01$), 15 ($P<0.001$ and $P<0.05$, respectively), and 20 ($P<0.01$ and $P<0.05$, respectively) p.i. but significantly decreased in the lungs at day 20 p.i. ($P<0.01$) in comparison of day 15 p.i.

## Discussion

In recent years, a critical role for Gal-9 has emerged in infectious disease, autoimmunity, and cancer (Merani et al. 2015). Accumulating evidence indicates that galectins fall into the category of immune regulatory molecules. Gal-9 ameliorates respiratory syncytial virus-induced pulmonary immunopathology through regulating the balance between Th17 and regulatory T cells (Lu et al. 2015). Gal-9 exerts its pivotal immunomodulatory effects by inducing apoptosis or suppressing effector functions via engagement with its receptor, Tim-3. Interaction of soluble Gal-9 with Tim-3 expressed on the surface of activated $CD4^+$ T cells renders them less susceptible to HIV-1 infection, while enhanced HIV infection occurs when Gal-9 interacts with a different receptor than Tim-3, indicating the versatile role of Gal-9 in viral pathogenesis (Merani et al. 2015). In addition, the plasma levels of Gal-9 appear to track dengue virus inflammatory responses and may serve as an important novel biomarker of acute dengue virus infection and disease severity (Chagan-Yasutan et al. 2013). In this study, we demonstrated that *Pb*ANKA infection induces the upregulation of Gal-9 and Tim-3 expressions in the lungs and MLNs.

Previous work from our laboratory has shown that KM mice may be a good alternative animal model for the study of lethal murine malaria (Huang et al. 2013). In this study, we successfully constituted a *Pb*ANKA-induced ALI in KM mice, dyspnea, or respiratory insufficiency occurred between 18 to 22 days p.i. before deaths. The lung tissue damages were observed from day 5 p.i.; histopathological examination showed that the major changes in the lungs of these mice were characterized by inflammatory cellular infiltration (mainly polymorphonuclear cells, lymphocytes, and mononuclear cells in the alveolar and interstitial sites), alveolar edema, and hemorrhage, with highly parasitized RBCs. In addition, the level of BALF total protein was increased in our animal model, which is indicative of alveolar-capillary membrane barrier disruption (Ware and Matthay 2000; Guidot et al. 2006).

Immunologic mechanisms are believed to play an important role in the pathogenesis of malaria-induced ALI, and the study of cells and molecules with immunoregulatory activity has begun to gain importance in recent years. Studies have highlighted the immunomodulatory properties of β-galactoside-binding protein, Gal-9, and its receptor Tim-3 in parasitic diseases (Katoh et al. 2012; Wu et al. 2014). Gal-9 can be highly modulatory for immune function depending on the circumstance (Wiersma et al. 2013), and some of this activity is mediated by the inhibitory molecule Tim-3 (Zhu et al. 2005). Although data about the role of Gal-9/TIM-3 pathway in the pathogenesis of human diseases is emerging, research about their role during malaria is scarce. In the present study, by using immunohistochemical technique, we found that the numbers of $Tim\text{-}3^+$ and $Gal\text{-}9^+$ cells in the lungs and MLNs of *Pb*ANKA-infected mice were significantly increased at all the times in comparison of uninfected controls; at the same time, the mRNA levels of Tim-3 and Gal-9 were significantly increased in the lungs and MLNs after infection. It has been reported that Tim-3 binding to Gal-9 stimulates anti-microbial immunity (Jayaraman et al. 2010). Administration of exogenous reGal-9 significantly ameliorates hepatocellular damage caused by liver ischemia and reperfusion injury in mice, which may be a new therapeutic strategy against innate immunity-dominated liver tissue damage (Hirao et al. 2015). In addition, our data showed that pro-inflammatory (TNF-α and IL-6) and anti-inflammatory (IL-10) cytokines were over-expressed in the lungs, and IL-6 and IL-10 were over-expressed in the MLNs after *Pb*ANKA infection. IL-10 is originally released by Th2 cells but now is found to be produced by other types of cells as well including B cells, macrophages, and Th1 cells (O'Garra and Vieira 2007). The activation of the immune system by antigens released by *P. falciparum* plays an important role in the induction and worsening of lung damage (Boulos et al. 1993). CD36 and Fyn kinase are critical mediators of malaria-induced lung endothelial barrier dysfunction in mice infected with *Pb*ANKA (Anidi et al. 2013). Therefore, although the actual regulatory mechanisms for the control of cell surface Gal-9 and Tim-3 were unknown, the increase of $Gal\text{-}9^+$ and $Tim\text{-}3^+$ cells as well as the enhancement of Gal-9 and Tim-3 expressions in *Pb*ANKA-induced ALI, which may play an important role in the development of ALI in murine malaria.

In conclusion, because the nature of the Tim-3/Gal-9 pathway in malaria is poorly defined, we studied their expression, immunological, and pathological relevance in a mouse model in the current study. Our data revealed the potential role of Tim-3/Gal-9 in *Pb*ANKA-induced ALI. Indeed, there were some limitations in this study, and more studies should be performed to validate these findings in lung injury of malarial models.

**Acknowledgments** Research reported in this publication was supported in part by the Natural Science Foundation of China (nos. 81271854 and 81471973), the Natural Science Foundation of Guangdong Province, China (no. S2013010016736), and the Science and Technology Planning Project of Guangdong Province, China (nos. 2013B021800043, 2014A020212108, and 2014A020212212).

## References

Anidi IU, Servinsky LE, Rentsendorj O, Stephens RS, Scott AL, Pearse DB (2013) CD36 and Fyn kinase mediate malaria-induced lung endothelial barrier dysfunction in mice infected with *Plasmodium berghei*. PLoS One 8(8):e71010

Boulos M, Costa J, Tosta C (1993) Pulmonary involvement in malaria (review). Rev Inst Med Trop São Paulo 35:93–102

Chagan-Yasutan H, Ndhlovu LC, Lacuesta TL, Kubo T, Leano PS, Niki T, Oguma S, Morita K, Chew GM, Barbour JD, Telan EF, Hirashima M, Hattori T, Dimaano EM (2013) Galectin-9 plasma levels reflect adverse hematological and immunological features in acute dengue virus infection. J Clin Virol 58(4):635–640

Chou FC, Shieh SJ, Sytwu HK (2009) Attenuation of Th1 response through galectin-9 and T-cell Ig mucin 3 interaction inhibits autoimmune diabetes in NOD mice. Eur J Immunol 39:2403–2411

Geng H, Zhang GM, Li D, Zhang H, Yuan Y, Zhu HG, Xiao H, Han LF, Feng ZH (2006) Soluble form of T cell Ig mucin 3 is an inhibitory molecule in T cell-mediated immune response. J Immunol 176(3): 1411–1420

Guidot DM, Folkesson HG, Jain L, Sznajder JI, Pittet JF, Matthay MA (2006) Integrating acute lung injury and regulation of alveolar fluid clearance. Am J Physiol Lung Cell Mol Physiol 291(3):L301–306

Hirao H, Uchida Y, Kadono K, Tanaka H, Niki T, Yamauchi A, Hata K, Watanabe T, Terajima H, Uemoto S (2015) The protective function of galectin-9 in liver ischemia and reperfusion injury in mice. Liver Transpl 21(7):969–981

Huang B, Liu M, Huang S, Wu B, Guo H, Su XZ, Lu F (2013) Expression of Tim-1 and Tim-3 in *Plasmodium berghei* ANKA infection. Parasitol Res 112(7):2713–2719

Jayaraman P, Sada-Ovalle I, Beladi S, Anderson AC, Dardalhon V, Hotta C, Kuchroo VK, Behar SM (2010) Tim3 binding to galectin-9 stimulates antimicrobial immunity. J Exp Med 207(11):2343–2354

Jones LA, Roberts F, Nickdel MB, Brombacher F, McKenzie AN, Henriquez FL, Alexander J, Roberts CW (2010) IL-33 receptor (T1/ST2) signaling is necessary to prevent the development of encephalitis in mice infected with *Toxoplasma gondii*. Eur J Immunol 40(2):426–436

Katoh S, Oomizu S, Niki T, Shimizu H, Obase Y, Korenaga M, Oka M, Hirashima M (2012) Possible regulatory role of galectin-9 on *Ascaris suum*-induced eosinophilic lung inflammation in mice. Int Arch Allergy Immunol 158(S1):58–65

Knapp S, Wieland CW, van't Veer C, Takeuchi O, Akira S, Florquin S, van der Poll T (2004) Toll-like receptor 2 plays a role in the early inflammatory response to murine pneumococcal pneumonia but does not contribute to antibacterial defense. J Immunol 172(5): 3132–3138

Lu X, McCoy KS, Xu J, Hu W, Chen H, Jiang K, Han F, Chen P, Wang Y (2015) Galectin-9 ameliorates respiratory syncytial virus-induced pulmonary immunopathology through regulating the balance between Th17 and regulatory T cells. Virus Res 195:162–171

Merani S, Chen W, Elahi S (2015) The bitter side of sweet: the role of Galectin-9 in immunopathogenesis of viral infections. Rev Med Virol 25(3):175–186

Mohan A, Sharma SK, Bollineni S (2008) Acute lung injury and acute respiratory distress syndrome in malaria. J Vector Borne Dis 45(3): 179–193

O'Garra A, Vieira P (2007) Th1 cells control themselves by producing interleukin-10. Nat Rev Immunol 7:425–428

Rabinovich GA, Toscano MA (2009) Turning 'sweet' on immunity: galectin-glycan interactions in immune tolerance and inflammation. Nat Rev Immunol 9:338–352

Reddy PB, Sehrawat S, Suryawanshi A, Rajasagi NK, Mulik S, Hirashima M, Rouse T (2011) Influence of galectin-9/Tim-3 interaction on herpes simplex virus-1 latency. J Immunol 187(11):5745–5755

Rodriguez-Manzanet R, DeKruyff R, Kuchroo VK, Umetsu DT (2009) The costimulatory role of TIM molecules. Immunol Rev 229:259–270

Rojo-Marcos G, Cuadros-González J, Mesa-Latorre JM, Culebras-López AM, Pablo-Sánchez R (2008) Case report: acute respiratory distress syndrome in a case of *Plasmodium ovale* malaria. Am J Trop Med Hyg 79:391–393

Seki M, Oomizu S, Sakata KM, Sakata A, Arikawa T, Watanabe K, Ito K, Takeshita K, Niki T, Saita N, Nishi N, Yamauchi A, Katoh S, Matsukawa A, Kuchroo V, Hirashima M (2008) Galectin-9 suppresses the generation of Th17, promotes the induction of regulatory T cells, and regulates experimental autoimmune arthritis. Clin Immunol 127:78–88

Taylor WR, Canon V, White NJ (2006) Pulmonary manifestations of malaria: recognition and management. Treat Respir Med 5:419–428

Taylor WR, Hanson J, Turner GDH, White NJ, Dondorp AM (2012) Respiratory manifestations of malaria. Chest 142(2):492–505

Ware LB, Matthay MA (2000) The acute respiratory distress syndrome. N Engl J Med 342(18):1334–1349

Wei J, Wu F, Sun X, Zeng X, Liang JY, Zheng HQ, Yu XB, Zhang KX, Wu ZD (2013) Differences in microglia activation between rats–derived cell and mice-derived cell after stimulating by soluble antigen of IV larva from *Angiostrongylus cantonensis in vitro*. Parasitol Res 112(1):207–214

White NJ, Pukrittayakamee S, Hien TT, Faiz MA, Mokuolu OA, Dondorp AM (2013) Malaria. Lancet 383(9918):723–735

Wiersma VR, de Bruyn M, Helfrich W, Bremer E (2013) Therapeutic potential of Galectin-9 in human disease. Med Res Rev 33(S1): E102–126

Wu B, Fu X, Huang B, Tong X, Zheng H, Huang S, Lu F (2014) Comparison of dynamic expressions of Tim-3 and PD-1 in the brains between toxoplasmic encephalitis-resistant BALB/c and -susceptible C57BL/6 mice. Parasitol Res 113(4):1261–1267

Zhao J, Endoh I, Hsu K, Tedla N, Endoh Y, Geczy CL (2011) S100A8 modulates mast cell function and suppresses eosinophil migration in acute asthma. Antioxid Redox Sign 14(9):1589–1600

Zhu C, Anderson AC, Schubart A, Xiong H, Imitola J, Khoury SJ, Zheng XX, Strom TB, Kuchroo VK (2005) The Tim-3 ligand galectin-9 negatively regulates T helper type 1 immunity. Nat Immunol 6(12): 1245–1252